

WAVE OVERTOPPING SIMULATOR TESTS ON TRANSITIONS AND OBSTACLES AT GRASS COVERED SLOPES OF DIKES

Gosse Jan Steendam¹, André van Hoven², Jentsje van der Meer³ and Gijs Hoffmans²

Previous tests performed with the Wave Overtopping Simulator showed that objects on dikes may impose a weak spot. To investigate this conclusion further, new wave overtopping tests have been performed in 2013, within the Dutch program SBW (Strength and Loads on Water Defences). These tests were particularly aimed at the influence of transitions between the soft cover layer of clay and grass and hard structures like asphalt and concrete. Specific tests were performed to determine the influence of transitions and objects on the critical velocity of the grass covered slope, which is used in the cumulative overload method. In addition pulling tests on grass were performed, using a new developed device. Further analysis may give a relationship with the critical velocity.

Keywords: Dikes, Wave Overtopping, Wave Overtopping Simulator, Grass cover, Grass pulling tests

INTRODUCTION

Since 2007 many tests were performed with the Wave Overtopping Simulator to investigate the stability of grass covered dike slopes. These tests contributed to the development of a new model quantifying loads and impacts by overtopping waves and the strength of landward grass covered slopes, the cumulative hydraulic overload model. This model will be implemented in design and assessment tools. From these tests it is known that the number of overtopping waves, in which the critical current velocity is exceeded, is one of the governing factors for cause of damage at the grass covered slope. Van der Meer et al. (2010) describes the cumulative hydraulic overload method including this critical velocity:

$$\sum(U_i^2 - U_c^2) = D \text{ [m}^2/\text{s}^2] \quad \text{for } U_i > U_c \quad (1)$$

Where:

U_i = the front velocity of overtopping wave i

U_c = the critical velocity of the grass slope (= strength of the grass slope)

D = damage number

N = the number of the waves in which $U_i > U_c$

These tests also showed that objects and transitions are often weak spots of the revetment. Within the extensive Dutch research program WTI 2017, financed by Rijkswaterstaat, new tests were performed with the Wave Overtopping Simulator, particularly aimed at the influence of transitions between the soft cover layer of clay and grass on dikes with hard structures like asphalt and concrete. Specific tests were performed to determine the critical velocity of the grass covered slope, which is used in the cumulative hydraulic overload model, and the influence of transitions and objects in that. To include the effects of transitions and obstacles on dikes Equation 1 was modified to (Deltares, 2013):

$$\sum(\alpha_M U_{i,\text{crest}}^2 - \alpha_s U_c^2) = D \text{ [m}^2/\text{s}^2] \quad \text{for } \alpha_M U_{i,\text{crest}}^2 > \alpha_s U_c^2 \quad (2)$$

The equation and the individual parameters will be explained in this paper.

WAVE OVERTOPPING SIMULATOR TESTS

In 2013, following previous test from 2007 to 2012 at various locations in the Netherlands and Belgium (a.o. Steendam et al., 2012), grass erosion tests have been performed on dikes at the river Rhine. One of the objective of these tests was to investigate the influence of hard structures (disturbing the flow and increasing the erosive impact) on grass and clay erosion at the transitions.

¹ Department Flood Defence, Infram International, P.O. Box 150, 3950 AD, Maarn, The Netherlands

² Deltares, P.O. Box 177, 2600 MH, Delft

³ Van der Meer Consulting bv, P.O. Box 11, 8490 AA, Akkrum, The Netherlands and UNESCO IHE, Westvest 7, 2611 AX, Delft, The Netherlands



Figure 1. Tested transition: from grass to concrete.

Tests with the Wave Overtopping Simulator (a.o. Van der Meer et al., 2008) were performed at two locations, at Nijmegen and Millingen. At the first location tests were performed on grass-concrete transitions (Figure 1) and a grass-gravel transition. At the second location Millingen the transition between a grass cover and an asphalt road on top of the dike was tested.

The objective of the tests at Nijmegen and Millingen was fourfold:

- To establish the resistance against erosion due to wave overtopping of the grass cover;
- To establish the influence of discontinuities on the resistance against erosion;
- To determine the critical current velocity of the grass cover (see also section on cumulative hydraulic overload);
- To measure the front velocity and the layer thickness of the overtopping water.

To realize these objectives, at both locations different test sections were used. Table 1 gives an overview.

Site	Test section	Test objective
Nijmegen	N-1	Determine the erosion resistance of a grass cover at the transition to a: <ul style="list-style-type: none"> - vertical concrete object along the test section (construction //); - gravel berm at the downstream end of the slope (geometrical transition); - concrete slab at the downstream end of the slope (revetment transition-concrete slab).
	N-2	Determine the erosion resistance of a grass cover at the transition to a: <ul style="list-style-type: none"> - gravel berm at the downstream end of the slope (geometrical transition) - vertical concrete beam at the downstream end of the slope (vertical wall structure).
	N-3	Determine the critical velocity
Millingen aan de Rijn	M-1	Determine the erosion resistance of a grass cover at the transition to an asphalt road on the crest (geometrical and revetment transition).
	M-2	Hydraulic measurements of the front velocities and layer thicknesses of overtopping water, determination of the critical velocity and measurement of the pressure gradients over the grass

A wave spectrum can be transformed into a wave overtopping distribution, depending on structure geometry and relative crest freeboard. The Wave Overtopping Simulator, mounted at the crest of a test section, releases overtopping wave volumes according to this distribution in a random order out of a tank which is continuously filled by pumps.

The test sections were four meters wide and were bounded by 0,5 m high guidance walls in order to keep the overtopping water within the test section.

At every test the impact of the overtopping wave volumes on the integrity of the grass covered slope and at the transitions was monitored closely. All tests were filmed and measurements of damages took place by hand as well as with 3D laser scans.

In every N-1 test, different wave overtopping discharges were exposed during 6 hours. Each test started with 6 hours of 1 l/s per m, then 6 hours of 10 l/s per m, 6 hours of 50 l/s per m, 6 hours of 100 l/s per m and finally 6 hours of 200 l/s per m. The last two sub-tests were slowed down because of an insufficient pump capacity (due to a lower expected water level in the river). Tests N-3 en M-2 were carried out differently, but these tests are not discussed further in this paper.

From previous tests at the Vecht dike (Steendam et al, 2012) it was learned that damage numbers (D) can be given with the cumulative hydraulic overload model (see next section):

$$\begin{aligned} \text{initial damage:} & & D < 500 \text{ m}^2/\text{s}^2 \\ \text{damage at various locations:} & & 500 \text{ m}^2/\text{s}^2 < D < 1500 \text{ m}^2/\text{s}^2 \\ \text{dike failure:} & & D > 3500 \text{ m}^2/\text{s}^2 \end{aligned}$$

Table 2 gives the test results as the required time to reach ‘damage at various locations’ ($D \approx 1000 \text{ m}^2/\text{s}^2$) and ‘failure of the grass’ ($D > 3500 \text{ m}^2/\text{s}^2$).

Table 2. Test results		
Location	Required time and overtopping amounts (reached in storm) to reach $D=1000 \text{ m}^2/\text{s}^2$	Required time and overtopping amounts (reached in storm) to reach $D=3500 \text{ m}^2/\text{s}^2$
(N-1)		
Undisturbed slope (1V:2H)	2.0 h - 50 l/s per m	1.0 h - 100 l/s per m
geom. transition	6.0 h - 10 l/s per m	4.0 h - 50 l/s per m
Construction //	2.5 h - 50 l/s per m	6.0 h - 50 l/s per m
Revet.transition berm-concrete slab	1.0 h - 100 l/s per m	n.a.
Nijmegen 2 (N-2)		
slope (1V:3H)	6.0 h - 100 l/s per m	1.5 h - 200 l/s per m
geom. transition	4.0 h - 50 l/s per m	4.0 h - 100 l/s per m
Vertical wall structure	1.0 h - 50 l/s per m	n.a.
Millingen 1 (M-1)		
slope	>6.0 h - 200 l/s per m	
geom. transition	5.0 h - 200 l/s per m	
Revet. Transition (road-grass)	6.0 h - 10 l/s per m	2.0 - 50 l/s per m
Revet. Transition (road-grass)	>6.0 h - 50 l/s per m	

CUMMULATIVE HYDRAULIC OVERLOAD METHOD AND MODIFICATION

This paper discusses the cumulative overload method and the required modification to incorporate a load increase or load decrease and/or a strength reduction due to transitions or obstacles (Deltares, 2013). The cumulative overload method is given as Equation 1. The damage number is determined by considering the number of waves and the flow velocities of the largest wave volumes as well as from

observations after the hydraulic measurements. In Van der Meer 2010 examples are given of corresponding damages in the field (Figure 2).



Initial damage ($D < 500 \text{ m}^2/\text{s}^2$)



Damage at various locations or multiple open spots ($500 \text{ m}^2/\text{s}^2 < D < 1500 \text{ m}^2/\text{s}^2$)



Failure ($D > 3500 \text{ m}^2/\text{s}^2$)



Non-failure after testing

Figure 2. Different definitions of damage and failure (Van der Meer et al. 2010)

To include the effects of transitions and obstacles on dikes Eq. 1 is modified, see Equation 2, where α_M is the load factor and α_s is the strength factor. The first term on the left side is a measure for the load and the second term represents the measure for strength. Equation 2 represents a hypothesis which is evaluated with the prototype experiments at Nijmegen and Millingen.

Flow velocity

For overtopping waves the flow velocity at the transition of the crest of the dike to the landward slope can be approximated by (SBW 2012-2).

$$U_{i,crest} = \alpha_v V_i^{\beta_v} \quad (3)$$

Where V is the overtopping wave volume (expressed in m^3) and $\alpha_v (= 4.5)$ and $\beta_v (= 0.3)$ are dimensional coefficients. The flow on the landward slope accelerates and can be computed with the model as developed by Schüttrumpf and Oumeraci (2005). A first estimation can be given, with α_a as an acceleration factor, by

$$U_{i,slope} = \alpha_a U_{i,crest} \quad (4)$$

The Nijmegen measurements showed that the erosion occurs faster if the slope is steeper than 1V:3H. The acceleration factor varies from 1.25 to 1.5 close to the toe of the dike. Hence, if the

velocity is calculated by using Eq. 4 then the magnitude of D obtained from the cumulative overload method increases with a factor of 3 to 6.

Load factor

The experiments show that erosion at revetment transitions (Fig. 3), at geometrical transitions (Fig.4) and at side-wall structures (e.g. at trees; Fig. 5) differs with respect to erosion at e.g. slopes or horizontal grass revetments. This difference can be ascribed to both an increase of the load and a reduction of the grass strength.



Figure 3. Revetment transitions from grass to asphalt and from asphalt to grass



Figure 4. Example Geometrical transition (earlier test at Kattendijke)



Figure 5. Erosion at tree (earlier test at Vecht dike);

Usually the load is expressed in forces which are proportional to the flow velocity squared. Defining:

$$\alpha_M = \frac{F_m}{F} = 1 + \frac{dF}{F} \quad (5)$$

where dF is the increase of the shear (or normal) force at the transition or obstacle; F which is related to $(U_i)^2$, represents the shear (or normal) force under flow conditions on a regular slope and F_m is the maximum shear (or normal) force. Hoffmans et al, 2014 and Deltares, 2013 discuss engineering methods for the erodibility of grass at transitions and objects on dikes whereas this paper back calculates α_M from the tests.

At transitions from a dike slope to a horizontal berm, a downward directed centripetal force acts at the transition which results in an increase of the normal force. At transitions from the horizontal crest to the inner slope the normal force reduces as the centripetal force is directed upwards. Also at side-wall structures there is a down-flow just before the stagnation zone giving an increase of the normal force at the bed.

For revetment transitions, the load increase is determined by the roughness difference of the beds. For geometrical transitions, the magnitude of the centripetal force depends on the steepness of the inner slope. For vertical objects and side-wall structures, the impact force is dependent on the geometry of the object.

Revetment transitions

Damage at various locations ($D = 1000 \text{ m}^2/\text{s}^2$) at the test location Millingen M-1 was measured at $t = 6 \text{ h}$ with 10 l/s per m ; failure near the transition ($D = 3500 \text{ m}^2/\text{s}^2$) was observed at 2 h with 50 l/s per m . With the following assumptions the predicted and measured times for both the ‘damage at various locations’ and for ‘failure’ are about in agreement:

- Typically, the clay quality near the edges is less fat as the clay cover on the undisturbed slope which can be ascribed to the sand layer below the asphalt road. Here these effects are not considered;
- Eddies, formed by the presence of the geometrical transition, i.e. from the horizontal crest to the landward slope, are neglected;
- Acceleration factor $\alpha_a = 1.0$ (see also Eq. 4);
- Load factor $\alpha_M = 1.75$;
- Critical flow velocity on slope $U_c = 4.5 \text{ m/s}$;
- Strength factor $\alpha_s = 0.9$ hence U_c reduces from 4.5 m/s to 4.0 m/s (see also Eq. 2).

Table 3 shows the calculated damage numbers of these events for three values of α_M . By using a load factor of $\alpha_M = 1.75$, the damage number D at $t = 6 \text{ h}$ with 10 l/s per m for ‘damage at various locations’ equals $771 \text{ m}^2/\text{s}^2$. For ‘failure of the grass cover’ the calculated damage number $D = 4,241 \text{ m}^2/\text{s}^2$. These calculated values of D are in agreement with the defined values as discussed in SBW-2012-2.

α_M (-)	U_c (m/s)	$t_{measured}$ (hours)	Damage at various locations $D \text{ (m}^2/\text{s}^2)$	$t_{measured}$ (hours)	Failure of grass cover $D \text{ (m}^2/\text{s}^2)$
1.50	4.0	6 h – $10 \alpha_s$	330	2 h – $50 \alpha_s$	2320
1.75	4.0	6 h – $10 \alpha_s$	771	2 h – $50 \alpha_s$	4241
2.00	4.0	6 h – $10 \alpha_s$	1436	2 h – $50 \alpha_s$	6690

If the load factor is reduced by the effects of a geometrical transition then the strength factor should also decrease (or U_c must decrease). This analysis has not been done here. The load factor for an asphalt road to a grass revetment lies in the range of 1.5 to 2.0 with a best guess value of $\alpha_M = 1.75$. The reduction of the strength, expressed by α_s is about 0.9. This value agrees approximately with the results of Pijpers (2013).

Although the computational results are in the range of the measured results, it is recommended to validate the theoretical modelling with more (prototype) tests. Therefore, it is needed to select

experiments where damage at transitions is/was observed. In addition, guidelines are needed for predicting the strength of different materials.

Geometrical transitions

Overtopping water acts like a water jet on the inner slope. At the transition of the slope to a horizontal berm the jet wants to follow its downward direction. Here the jet impact area is transformed into an energy dissipater and a scour hole is formed. Figure 6 shows a scour hole at the toe of the dike due to wave overtopping. Note that when a scour hole is formed deeper than 20 cm the grass revetment fails.



Figure 6. Scour hole at the toe of the dike; the sub soil consists of gravel (Kattendijke)

For geometrical transitions as shown in Fig. 6 the load factor (α_M) can be written as function of the steepness (θ), (SBW-2012-2)

$$\alpha_M = 1 + \sin \frac{1}{2}\theta \quad (6)$$

If there is no geometrical transition or if $\theta = 0^\circ$ then $\alpha_M = 1$. If $\theta = 20^\circ$ (steepness is 1V:2.7H) then $\alpha_M = 1.17$. In SBW-2012-2 predictions were given for the load factor. These predictions were based on a scour approach and therefore they are less reliable. Nevertheless, Eq. 6 gives similar results as in the predictions for slopes with a steepness of 1V:3H. For a steeper slope, say 1V:2H, the load factor obtained from Eq. 6 is 10% smaller than the predicted value.

By using both the experimental data and the cumulative overload method values for the load factor were calculated, and a variation was found between 1.25 to 1.35 for Nijmegen (N1 and N2) (see Table 4). For the steepest slope (N1) the load factor was found to be 1.35. In the Millingen tests it was observed that ‘damage at various locations’ occurred at the same time at the undisturbed slope and at the geometrical transition, because the water could not flow away from the scouring hole. Most likely this pool influenced/reduced the erosion process. Therefore, the load factor is $\alpha_M \approx 1$. By using Eq. 6 the predicted load factor lies in the range of 1.16 (Nijmegen N2) to 1.23 (Nijmegen N1).

Table 4. Load factor at the geometrical transition for Nijmegen and Millingen (U_c is related to crest conditions)						
Location	α_M (-)	U_c (m/s)	$t_{measured}$ (hours)	Multiple open spots D (m^2/s^2)	$t_{measured}$ (hours)	Failure grass cover D (m^2/s^2)
Nijmegen (N1) -slope-	1.00	3.5	1.5 h – 50 α_s	734	6.0 h – 50 α_s	2636
Nijmegen (N1) -toe-	1.23	3.5	6.0 h – 10 α_s	376	4.0 h – 50 α_s	4324
Nijmegen (N1) -toe-	1.35	3.5	6.0 h – 10 α_s	613	4.0 h – 50 α_s	6061
Nijmegen (N2) -slope-	1.00	4.5	4.0 h – 100 α_s	959	1.5 h – 200 α_s	3280
Nijmegen (N2) -toe-	1.16	4.5	4.0 h – 50 α_s	361	4.0 h – 100 α_s	1589
Nijmegen (N2) -toe-	1.25	4.5	4.0 h – 50 α_s	600	4.0 h – 100 α_s	3977

Although there are differences between the measured and calculated load factors the relative error is less than 10%. The range of the load factor obtained from Eq. 7 is in agreement with other prototype measurements (see also SBW 2012-1). If the flow direction changes at the transition from a horizontal crest to an inner slope then the load factor is:

$$\alpha_M = 1 - \sin \frac{1}{2}\theta \quad (7)$$

It is recommended to validate this theoretical equation with more prototype experiments.

Vertical objects and side-wall structures

At the test site in Nijmegen, a side-wall structure was tested on the horizontal berm as shown in Fig. 7. In the stagnation zone the grass revetment was reinforced with a concrete protection in order to prevent erosion at that location. However, in the acceleration zone 'damage at various locations' was observed very early at $t = 1$ h with $q = 50$ l/s. Subsequently, the acceleration zone was covered with a geotextile. The load factor at side-wall structures was found to be $\alpha_M = 1.7$, with a critical flow velocity $U_c = 4.5$ m/s and a strength factor $\alpha_s = 1.0$.

Hence, the calculated time t in which initial damage occurred, is 1 h (with $q = 50$ l/s giving $D = 997$ m²/s²), see Table 5.

α_s (-)	α_s (-)	α_M (-)	U_c (m/s)	$t_{measured}$ (hours)	Multiple open spots D (m ² /s ²)
1.0	1.0	1.4	4.5	1 h – 50 α_s	338
1.0	1.0	1.7	4.5	1 h – 50 α_s	997
1.0	1.0	2.0	4.5	1 h – 50 α_s	2102
1.0	1.0	2.3	4.5	1 h – 50 α_s	3657

At the test site in Nijmegen, the dimensions of the side-wall structures were relatively small. Hence, additional research is needed for validation of the parameters for bigger objects like houses or other (hydraulic) structures which can be found on dikes. And there are more knowledge gaps, e.g. close to stairs the strength (or weakness) of the transition still cannot be determined analytically, (Fig. 8).



Figure 7. Side-wall structure



Figure 8. Erosion close to stairs (Tholen)

GRASS PULLING DEVICE

With overtopping simulator tests the knowledge about the flow velocity and the flow thickness on slopes induced by overtopping waves as well as the strength and flow resistance of grass at undisturbed slopes and at transitions, increased enormously. For safety assessments it would be practical if one could determine the critical velocity, the strength of the grass cover, in an easier manner. One option could be to determine the condition of the grass cover by an inspection and relate the findings to a critical velocity. But an inspection alone is not sufficient; it will remain necessary to determine the actual strength. A first attempt to measure the grass strength in situ has been performed with a new developed grass sod pulling device.

A grass sod consists of soil and roots where the roots can be considered as anchors for the grass and a reinforcement mesh in the soil. As roots are not straight but grow subdivided in the sub-soil, the grass sod can be deformed centimetres without tearing. Pressures acting on the grass cover can stretch and break at first the weakest roots. The breaking of a few roots will weaken the grass, but the forces will easily redistribute to other roots. However, the redistribution stops when a critical amount of roots is broken at the critical value of displacement.

This phenomena was also observed during wave overtopping tests. It was noticed that the grass cover did not fail suddenly at one large overtopping wave, but due to several relative smaller overtopping volumes where the volume at failure was not necessarily the largest.

In April 2013 Infram carried out 24 grass pulling tests at the dike in Millingen and 24 tests in Nijmegen at different locations for unsaturated soil conditions. In these tests the tensile force as function of the deformation was measured at different locations on the dike. The forces and deformations were measured with a force transducer and a displacement meter, respectively. The force-deformation curve was analyzed in relation to the strength of the grass sods. Also the influence of fatigue on the strength of grass was investigated.

Tests with the new developed grass pulling device are carried out as follows. First a U-frame with dimensions of 5 cm x 15 cm x 15 cm was gradually pushed in the sub soil. Next, the soil was carefully removed with a small spade either on four sides (Condition A) or on two sides (Condition B). So in condition A there is no additional strength from the sides and in condition B there is additional strength from two sides. Finally, after the soil sample was anchored by horizontal pins at about 3 cm below the surface (see Fig. 9), the pulling test on the frame started.



Figure 9. Grass pulling test device

The maximum deformation of the grass sod is extremely high, i.e. approximately 6 cm. However, the tensile force reaches its maximum value after 5 mm to 10 mm deformation. Figure 10 shows an example of the deformation as a function of the tensile force. The grass sod was deformed gradually until the grass sod failed completely. In these tests the grass sod was pulled up with a constant speed in the order of 1.5 cm/s. During the experiments we could continuously hear the tearing of roots. Hence, short roots break in the beginning of the tests and longer ones later.

Condition A tests at Millingen test site showed that the maximum tensile force varied from 0.21 kN to 0.55 kN. Condition B tests showed an increase of the maximum tensile force to a range from 0.41 kN to 0.95 kN. For grass on the test site Nijmegen similar results were obtained. These forces are relatively large as they can easily lift stones with dimensions of 15 cm x 15 cm x 50 cm. However, this comparison is not correct as the influence of the fatigue strength of grass has not yet been included.

The strength factor α_s is a factor to model the reduction of the grass strength at revetment transitions. Since the maximum tensile forces are measured for two test conditions, α_s can be determined by using the following equation (Deltares, 2013):

$$\alpha_s = \frac{1.5F_{m,B} - 0.5F_{m,A}}{2F_{m,B} - F_{m,A}} \quad (8)$$

in which $F_{m,A}$ is the maximum force for condition A (no additional strength from the sides) and $F_{m,B}$ represents the maximum force for condition B (additional strength on two sides). Based on about 20 experiments the strength factor ranges from 0.81 to 0.97 with a mean value of $\alpha_s = 0.9$.

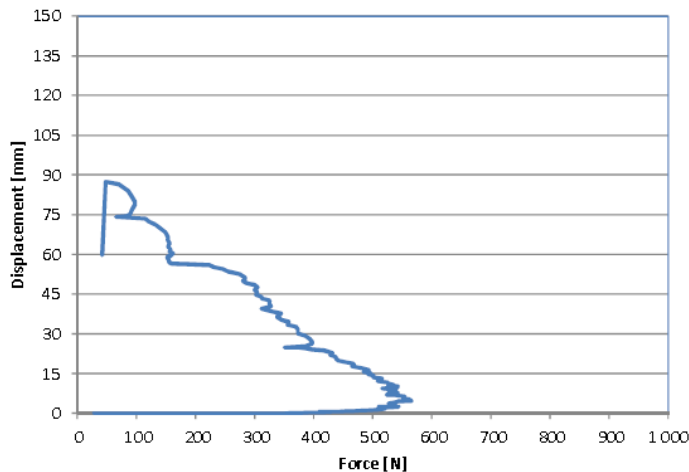


Figure 10. Deformation as function of force

Fatigue strength

Fatigue is the progressive and localized structural damage that occurs when a material is subjected to cyclic loading. Fatigue strength is an expression used to describe a property of a material: the amplitude (or range) of cyclic stress that can be applied to the material without causing fatigue failure. Typically, the fatigue strength is defined as the value of stress at which failure occurs after N_f cycles.

Also fatigue tests were performed to analyze the elastic and plastic behaviour of the grass sod (Fig. 11). In these experiments, repeatedly a deformation step of 0.5 cm was applied until failure of the grass sod occurred. After each deformation step the load was reduced. The loading and unloading were repeated continuously. After a series of 5 deformation steps the deformation was increased with 0.5 cm (from 0.5 cm to 1.0 cm and so on). A total number of approximately 60 load repetitions was carried out as the maximum deformation was about 6 cm, as can be seen in Fig. 12.

The fatigue tests showed that after a deformation of 20 mm (or after 20 load repetitions) the maximum tensile force was reached. This deformation is about two times larger than the deformation when the maximum tensile force occurred in the gradual deformation tests. This relation is not examined here in greater detail. Moreover, it is recommended to investigate the elastic and plastic behaviour of the grass sod. In the prototype situation when the grass revetment is loaded by the overtopping waves on the landward slope, the deformations are most likely less than 10 mm because of the high frequency pressure fluctuations. As the eddies with the highest energy have a period of about 0.03 s (or a frequency of 30 Hz) the maximum values of the measured tensile forces are representative for determining the critical flow velocity.

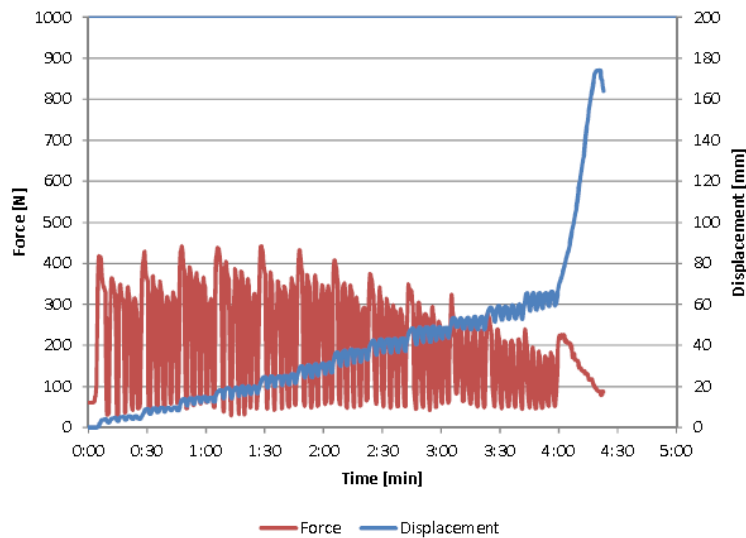


Figure 11. Force and displacement against time

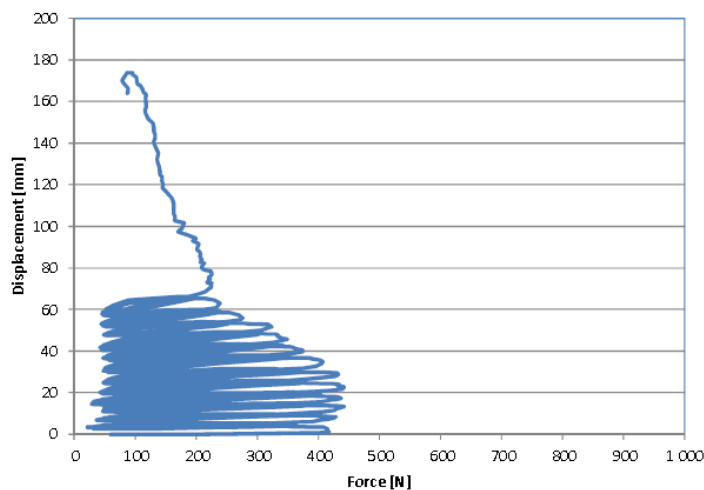


Figure 12. Displacement against force

Figures 11 and 12 show an example of the results of a fatigue test, i.e. force as function of time, deformation as function of time and deformation as function of force.

The number of cycles that grass can endure before it fails, is a complex function of the static and cyclic stress values, the root properties, the soil heterogeneity or the root area ratio, effective soil cohesion and several other factors. Although various grass cover-tensile tests were conducted during the winter period of 2013, the fatigue properties of the grass cover are still not fully understood. Measurements show that the tensile force decreases with an increase of the number of loads (see also Fig. 12). However, at present no fatigue curve of the grass sod is available.

CONCLUSIONS

In this paper the cumulative overload method and the required modification to incorporate a load increase or load decrease and/or a strength reduction due to transitions or obstacles was discussed. In 2013 prototype tests were performed in Nijmegen and Millingen with the objective to investigate the influence of hard structures on grass and clay erosion at the transitions. When a flow is aimed to the surface the load factor is greater than 1. The load decreases if there is an up-flow. The reduction of the strength is modeled in equation 2 by a strength factor which reduces the critical depth-averaged flow velocity. From the prototype tests a back calculation was made to calculate the load and the strength

factor. In SBW 2012-2, and Hoffmans et al, 2014 the theoretical modeling and derivation of values of the factors is discussed. The back calculation leads to values found as listed in Table 6.

Table 6. Values for load an strength factor for prototype tests		
	best guess α_M	best guess α_S
revetment transitions	1.75	0.9
geometrical transitions	1.35	1.0
Vertical objects	1.7	1.0

The range of the load factor obtained agrees with other prototype measurements and first modelling efforts (SBW 2012-2 and Hoffmans et al, 2014). It is remarked that the cumulative overload method will be evaluated by using all the experiments conducted from 2007 (including the wave run-up tests). In addition, the experimental results with respect to the transitions and objects should be evaluated in relation to the cumulative overload method and the engineering tools as discussed in SBW, 2012-2 and Hoffmans et al, 2014.

Knowledge about the flow velocity and the flow thickness on slopes induced by overtopping waves increased enormously with the tests with the Wave Overtopping Simulator. Also a lot of knowledge was gained on strength and flow resistance of grass at undisturbed slopes and at transitions. To estimate the strength of grass covers and the influence till now the use of the Wave Overtopping Simulator was needed. To gain even more knowledge to model physical processes and validate these models more experiments will be needed. But in the end for safety assessments it would be practical if one could determine the critical velocity, the strength of the grass cover and the influence of objects and transitions, in an easier manner. One option could be to determine the actual strength in situ with a new developed grass sod pulling device.

In April 2013 48 grass pulling tests were performed at different locations for unsaturated soil conditions. The maximum deformation of the grass sod was found to be extremely high, i.e. approximately 6 cm. However, the tensile force reached its maximum value after 5 mm to 10 mm deformation. Based on about 20 experiments a strength factor a mean value of $\alpha_s = 0.9$ was found.

Also fatigue tests were performed to analyze the elastic and plastic behaviour of the grass sod. The fatigue tests showed that after a deformation of 20 mm (or after 20 load repetitions) the maximum tensile force was reached. It was recommended to investigate the elastic and plastic behaviour of the grass sod.

In the prototype situation the deformations by overtopping waves are probably less than 10 mm. The fatigue properties of the grass cover are still not fully understood.

ACKNOWLEDGMENTS

Development and research was commissioned by the Dutch Rijkswaterstaat (WVL). The work was carried out within the WTI2017 program research & development of flood defence assessment tools. The research was performed by a consortium of partners and was led by Deltares. Consortium partners were Deltares (project leader, geotechnical issues, model descriptions), Infram (logistic operation of testing, hydraulic measurements and grass pull tests), Alterra (grass issues) and Van der Meer Consulting (performance of wave overtopping simulator, model descriptions and hydraulic measurements).

REFERENCES

- Deltares, 2013, Evaluation and Model Development - Grass Erosion Test at the Rhine dike, 1207811-002, 1207811-002-HYE-0007-svb, December 2013, DRAFT.
- Hoffmans, 2014, G.J.C.M., A. van Hoven, B. Harderman, H.J. Verheij Erosion of grass covers at transitions and objects on dikes, to be presented at Int. Conf. of Scour and Erosion, Perth
- Infram, 2013. Factual Report. Overslagproeven Rivierenland. Report 12i071, 19-06-2013.[in Dutch only]
- Pijpers, R., 2013, Vulnerability of Structural Transitions in Flood Defences, erosion of grass covers due to wave overtopping, M.Sc. thesis

- SBW, 2012-1. SBW Wave overtopping and grass cover strength. Model development. Deltares report 120616-007, June 2012. Authors: Gosse Jan Steendam, Gijs Hoffmans, Jan Bakker, Jentsje van der Meer, Joep Frissel, Maurice Paulissen and Henk Verheij.
- SBW, 2012-2. SBW Wave overtopping and grass cover strength. Predictions of Prototype Tests. Deltares report 120616-007, November 2012.
- Schüttrumpf, H.F.R. and H. Oumeraci, 2005. "Layer thicknesses and velocities of wave overtopping flow at seadikes." *Coastal Engineering*, 52, 6, pp.473–495.
- Schüttrumpf, H.F.R. 2001. Wellenüberlaufströmung bei See-deichen, Ph.D.-thesis, Technical University Braunschweig.
- Steendam G.J. , Y. Provoost and J.W. van der Meer, 2012,.Destructive wave overtopping and wave run-up tests on grass covered slopes of real dikes, *Proceedings International Conference on Coastal Engineering, ICCE 2012*, Santander, Spain
- Steendam G.J., P. Peeters, J.W. van der Meer, K. van Doorslaer and K. Trouw, 2011. Destructive wave overtopping tests at Flemish dikes, *proc. Coastal Structures 2011*, Yokohama, Japan
- Steendam, G.J., J.W. van der Meer, B. Hardeman and A. van Hoven, 2010. Destructive wave overtopping tests on grass covered landward slopes of dikes and transitions to berms, *Proc. ICCE 2010 Shanghai*, ASCE, China.
- Steendam, G.J., J.W. van der Meer, G. de Raat, W. de Vries and J.Y. Frissel, 2008. Influence of Management and Maintenance on erosive impact of wave overtopping on grass covered slopes of dikes. *International Symposium on Floodrisk 2008*. Oxford, United Kingdom.
- Van der Meer, J.W., P. Bernardini, W. Snijders and H.J. Regeling. 2006. The wave overtopping simulator. ASCE, ICCE 2006, San Diego, pp. 4654 - 4666.
- Van der Meer, J.W., P. Bernardini, G.J. Steendam, G.J. Akkerman and G.J.C.M. Hoffmans. 2007. The wave overtopping simulator in action. *Proc. Coastal Structures*, Venice, Italy.
- Van der Meer, J.W., G.J. Steendam, G. de Raat and P. Bernardini. 2008. Further developments on the wave overtopping simulator. ASCE, *Proc. ICCE 2008*, Hamburg, 2957-2969.
- Van der Meer, J.W., R. Schrijver, B. Hardeman, A. van Hoven, H. Verheij and G.J. Steendam. 2009. Guidance on erosion resistance of inner slopes of dikes from three years of testing with the Wave Overtopping Simulator. *Proc. ICE, Coasts, Marine Structures and Breakwaters 2009*, Edinburgh, UK.
- Van der Meer, J.W., B. Hardeman, G.J. Steendam, H. Schüttrumpf and H. Verheij. 2010. Flow depths and velocities at crest and inner slope of a dike, in theory and with the Wave Overtopping Simulator. ASCE, *Proc. ICCE 2010*, Shanghai.